

Synthesis, characterization and biological activity of some isoxazole derivatives via 1,3-dipolar cycloaddition reaction of nitrile oxide

Received: 23/05/2023

Accepted: 08/06/2023

Sarbast M. Ahmed¹ Hayman Sardar Abdulrahman¹ Faiq H. S. Hussain² Hiwa Omer Ahmad^{1*} Idrees B. Qader¹ Hemn A. Qader¹

Abstract

Background and objective: Isoxazoles are significant heterocyclic products that are used in various applications in the field of medicinal chemistry. Along with prescription drugs, a variety of bioactive pharmaceutical substances, such as valdecoxib, leflunomide, and danazol, include the isoxazole core. The present work aimed to synthesize and test the antibacterial, antioxidant, and antifungal activities combined with the theoretical investigations.

Methods: Various 2,4-disubstituted isoxazoles have been synthesized through a 1,3-dipolar cycloaddition reaction via nitrile oxide. The structures of synthesized compounds were fully characterised by multinuclear NMR spectroscopy. Anti-bacterial activity was investigated against *Escherichia coli* and *Staphylococcus aureus* by Muller Hinton agar using agar diffusion method. The biological effect of the synthesized compounds was investigated with the docking study.

Results: Herein, nine new target compounds were synthesized in moderate to high isolated yield. Naphthalene and chlorophenyl isoxazole substitutes have been found to enclose a higher effectiveness against bacterial, fungus and radical scavenging abilities based on the docking binding site energy. Compounds 5a-e exhibited various antibacterial activities against *Escherichia coli* as gram-negative bacteria ranging from 21 to 40 mm of the inhibitory zone (30 µg). The compound 5e exhibited a significant antioxidant activity using the 1,1-diphenyl-2-picrylhydrazyl radical (DPPH) (97.8 %). A range of docking energy scores between -9.4 and -13.7 Kcal/mol were observed for the compounds 5a-g and 9a-c.

Conclusion: The newly synthesized 2,4-disubstituted isoxazole compounds could serve as potent leads for the development of antimicrobial agents.

Keywords: Antibacterial; Antioxidant; 1,3-Dipolar Cycloaddition; Insilico; Isoxazole derivatives

Introduction

Isoxazole is a five-membered heterocycle that contains two heteroatoms, the oxygen and nitrogen atoms, which are located next to each other in the isoxazole structure. The unsaturated molecule properties can be attributed to the presence of two double bonds between carbon atoms. The isoxazole structure allows for many non-covalent interactions, including hydrophilic interactions (general hydrophilic profile with Clog *P* = 0.121), pi-pi stacks

(an unsaturated five-membered ring), and hydrogen bonds (where N and O atoms act as hydrogen bond acceptors).⁽¹⁾

Isoxazoles are important heterocyclic molecules that are used in many applications in the field of chemistry, particularly medicinal chemistry. Many bioactive medicinal compounds, including valdecoxib, leflunomide, and cloxacillin, in addition to prescription medications, contain the isoxazole core (Scheme 1).⁽²⁾

The addition of isoxazole could be

¹ Department of Pharmaceutical Chemistry, College of Pharmacy, Hawler Medical University, Erbil, Iraq.

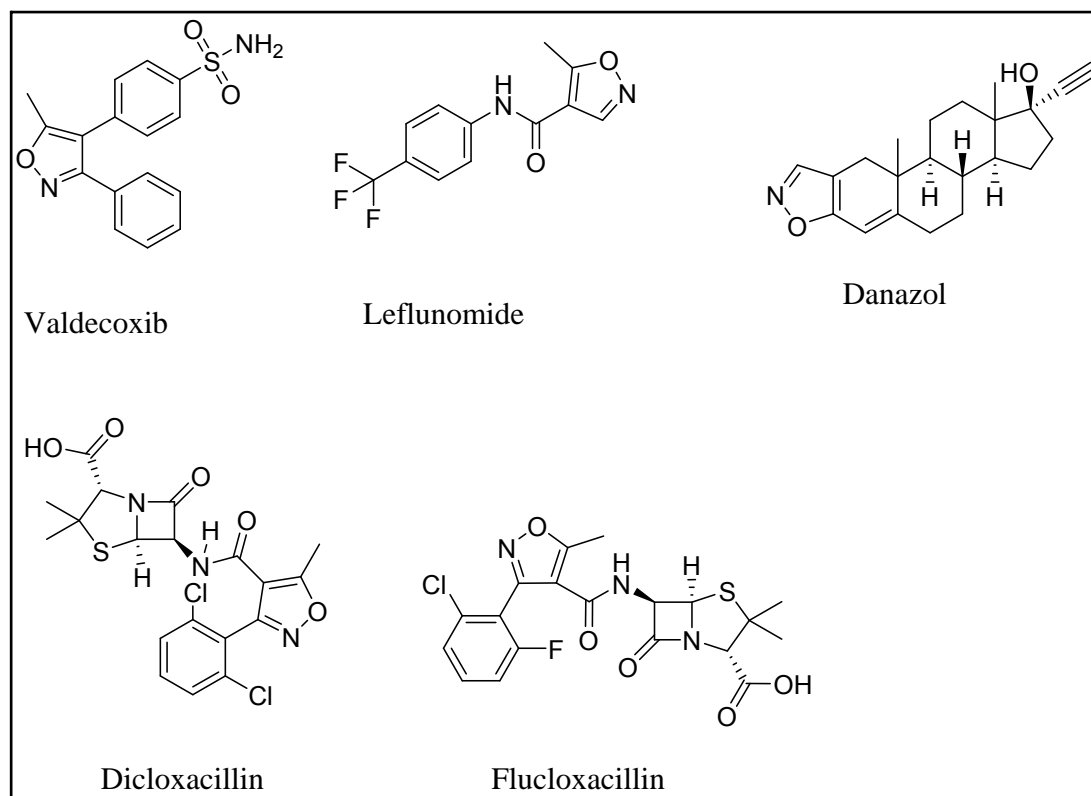
² Department of Medical Analysis, Faculty of applied Science, Tishk International University, Erbil, Iraq.

Correspondence: hiwa.omar@hmu.edu.krd

Copyright (c) The Author(s) 2022. Open Access. This work is licensed under a [Creative Commons Attribution-NonCommercial-ShareAlike 4.0 International License](https://creativecommons.org/licenses/by-nc-sa/4.0/).

responsible for increased efficacy, less toxicity, and better pharmacokinetic characteristics. Isoxazole compounds can interact with several protein targets with a broad range display of biological effects, including significant potential as antidepressants,⁽⁴⁾ antibacterial agents,^(5,6) immunosuppressants,⁽⁷⁾ anticancer agents,⁽⁸⁾ analgesics,⁽⁹⁾ anti-inflammatory agents,⁽¹⁰⁾ and antiviral agents,⁽¹¹⁾ The substitution of different groups on the isoxazole ring was responsible for their different activities. Several synthetic processes have been reported for forming the isoxazole core. Traditional techniques include reactions between α , β -unsaturated carbonyl and hydroxylamine compounds, or the α , β -unsaturated nitriles and 1,3-dicarbonyl compounds. Additionally, this family of compounds can be synthesised using 3+2 cycloaddition reactions between nitrile oxides and alkynes.⁽¹²⁾ Infectious diseases, in addition to war and famine, have long been considered the greatest obstacles to

human survival and progress. They are ranked among the world's primary causes of mortality and disability.⁽¹³⁾ Though bacterial infections can be controlled by the use of antibiotics, there has been an increasing prevalence of multidrug-resistant organisms.⁽¹⁴⁾ Antibiotic misuse, including self-medication, unrestricted access to medicines without a prescription, and noncompliance are the main factors that have led to a rise in antibiotic resistance.⁽¹⁵⁾ Another significant factor is the widespread misuse of antibiotics by the agricultural and poultry industries that continuously release antibiotics into the environment through wastewater, subsequently leading to their accumulation in the food chain.⁽¹⁶⁾ Herein, we present the theoretical docking and practical study of anti-bacterial and antioxidant activities of synthesized stable isoxazole derivatives via nitrile oxide, 1,3-dipolar cycloaddition reaction.



Scheme 1 Structures of isoxazoles exhibiting biological or pharmaceutical activities⁽³⁾

Methods

Chemistry

The present investigation was performed at postgraduate laboratory /Hawler Medical University/college of pharmacy. Melting points were recorded using electrothermal 9100. Infrared spectra were recorded in the range 4000-400 cm^{-1} using JASCO 4600 Scientific Instruments; all absorptions are expressed in cm^{-1} . ^1H -NMR and ^{13}C -NMR spectra were recorded on the Brukeravance (600 MHz) spectrometer (Day Petronic Company, Iran). Chemical shifts are expressed in parts per million downfield from tetra-methylsilane as an internal standard. NMR spectra were recorded in solutions in deuterated dimethylsulfoxide (DMSO-d_6). The solvents and reagents were purchased from commercial suppliers and used without further purification. The reactions were monitored by TLC, run on silica gel plates and then visualised with UV light. Column chromatography and TLC: silica gel H60 and GF₂₅₄, respectively; eluents: A mixture of cyclohexane/ethyl acetate 8:2.

Synthesis of ether derivatives 3a-g

A mixture of 4-hydroxybenzaldehyde substituted phenols (0.05mmol) and K_2CO_3 (0.11 mmol) was dissolved in 10 mL of absolute ethanol and stirred at room temperature for 2 hours. (0.05 mmol) of Propargyl bromide was added to the mixture and heated under reflux for 24 hours. The mixture was powered into ice and filtered, and the products were recrystallized from the diethyl ether (Scheme 2).⁽¹⁷⁾

Synthesis of 9-anthracenenitrile oxide 6

9-anthracenenitrile oxide 6 was prepared by dissolving 3.56 g (16.09 mmol) of 9-Anthraldehyde oxime 4 in 250 mL of chloroform along with 1.33mL (16.41 mmol) of pyridine. The solution was then cooled down to 0°C with an ice bath. Next, N-Chlorosuccinimide 2.02g (15.12 mmol) was added portion-wise, after stirring the mixture for three hours, and the organic phase was washed with water (3X100 mL) and then dried over anhydrous Na_2SO_4 .

Then, the solvent was evaporated and the product was recrystallized from Di-isopropyl ether (Scheme 3).⁽¹⁸⁾

Synthesis of ether functionalized isoxazoles 5a-g

To a stirred solution (0.01 mmol) of the prepared ether derivatives 3a-g in (50 mL) anhydrous DCM, (0.01 mmol) of the prepared 9-anthracennitrile oxide 6 was added portion wise. The reaction mixture was left under stirring at room temperature for 48 hours. After completion, it was washed with brine (3X50) and the organic layer was dried over anhydrous Na_2SO_4 . The solvent was then removed and the synthesised products were purified by column chromatography (Scheme 2).⁽¹⁹⁾

Synthesis of amine functionalized isoxazoles 9a-c

A mixture of (0.01 mmol) of amines and (0.01 mmol) of 3-(anthracen-9-yl)-5-(bromomethyl) isoxazole 7 in 20 mL DMSO was stirred at room temperature for 24 hours, the presence of (0.01 mmol) sodium bicarbonate. After completion, poured into crushed ice and organic products extracted with DCM (30 mL \times 3); the solvent was evaporated to give crude products which were purified by column chromatography by using a mixture of 8:2 cyclohexane: ethyl acetate (Scheme 4).⁽²⁰⁾

Determination of antibacterial activity

Two distinct microorganisms, *Escherichia coli* and *Staphylococcus aureus* were tested against each synthesised compound using the disc agar diffusion method by Muller Hinton agar. The inhibition zones and minimum inhibitory concentrations were determined using the agar well-diffusion method for the preservation of pure culture, sterilized by autoclave, and then poured into a Petri dish with a depth of 4 mm. In a nutshell, the nutrients agar medium (75 mL) was combined with the broth culture of the test strain at 37°C for 24 hours, thoroughly mixed, and then the plates were inoculated. After allowing the medium to settle, the discs of the synthesised compounds were mixed with KBr powder (1:3). The mixture was

pressed under pressure KBr, which has been used as a blank disc. The dried surface of the Muller Hinton agar plate was streaked; tow dried discs were placed on the surface of the cultured media per petri dish. The plates were then incubated at 37° C for 18 to 24 hours and, after the inhibition zone, were manually measured in mm (Table 5).⁽²¹⁾

Antifungal Activity

The sabouraud dextrose agar medium plate disc diffusion method was employed to assess the antifungal activity at a concentration of 50 µg per disk.⁽²²⁾ The antifungal activity of each synthesised isoxazole derivative was examined in vitro against *Candida albicans*. To get the ideal concentration, each synthesised compound was dissolved in DMSO. The discs (6 mm in diameter) were impregnated, air-dried and placed on the sabouraud dextrose agar media, which was previously seeded with 0.2 mL of a broth culture of each organism for 18 hours. Nearly 250 µL of samples of different concentrations were then filled in wells. The inhibitory zones were measured in millimetres after the plates had been incubated at 37°C for 24 hours; the activity results are shown in (Table 6).

Antioxidant activity

The percentage of antioxidant activity (AA %) of the prepared compounds, namely 5a-g were assessed by 1,1-diphenyl-2-picrylhydrazyl radical (DPPH). A PerkinElmer precisely Shelton, CT 06484 USA Lambda 25 UV/VIS spectrometer was applied for all UV-Vis absorption measurements (Figure 1). The evaluation of the DPPH free radical assay was determined at 517 nm after 12 hours of reaction according to Garcia *et al.*⁽²³⁾

$$AA\% = 100 - \left[\frac{(\text{Abs}_{\text{sample}} - \text{Abs}_{\text{blank}}) \times 100}{\text{Abs}_{\text{control}}} \right] \dots \text{Eq.1}$$

Molecular docking

The two-dimensional (2-D) structures of the ligand molecules were built using ChemDraw professional 16.0, converted to 3-dimensional (3-D) structures using

Chem3D 16.0 module and then saved in PDB format structures (<http://www.cambridgesoft.com/>). The ligand was optimised by adding Geister charges and hydrogen. The PDBQT format of the ligands was prepared with AutoDock Tools 1.5.7. The ligand molecules were then used as input for AutoDock Vina (<https://vina.scripps.edu/>) to carry out the docking simulation.

The X-ray crystal structure of the target of *Candida albicans* dihydrofolate reductase (ID:1AI9) for antifungal, beta-ketoacyl-ACP synthase-III (PDB ID:1HNJ) for antibacterial, Alpha-amylase from *Bacillus subtilis* (PDB ID: 1BAG) for antibacterial, alpha-sterol demethylase (CYP51) from *M. Tuberculosis* (PDB ID: 1EA1) for antitubercular activity,⁽²⁴⁾ and prepared active compounds such as potential antioxidants (PDB code: 2X08)⁽²⁵⁾ were retrieved from the RCSB Protein Data Bank web server (<http://www.rcsb.org/pdb/>). The active binding sites were identified, and the grid dimensions were set according to the coordinates x, y and z, for the target active binding sites identified in Discovery Studio Visualizer 2021.

The water molecules were removed from the receptors and polar hydrogen and Kollman charges were added. The PDBQT format of the receptors was generated by AutoDock Tools 1.5.7. AutoDock Vina was compiled and run under Windows 10.0 Professional operating system. Discovery Studio 2021 was used to deduce the pictorial representation of the interaction between the ligands and the target protein. The binding affinity (ki) of ligands for the selected targets was calculated using Eq. 2.

$$Ki = e^{(\Delta G / (R \times t))} \dots \dots \dots \text{Eq. 2}$$

Where ΔG is the binding energy in kcal/mol, the universal gas constant R = 1.987 kcal/K/mol and at room temperature (25°C) T = 273 + 25 = 298 K. Ki is the inhibition constant where Ki principally depends on the binding (or association) constant (K_b) having a unit of mM.⁽²⁶⁾

Results

Chemistry

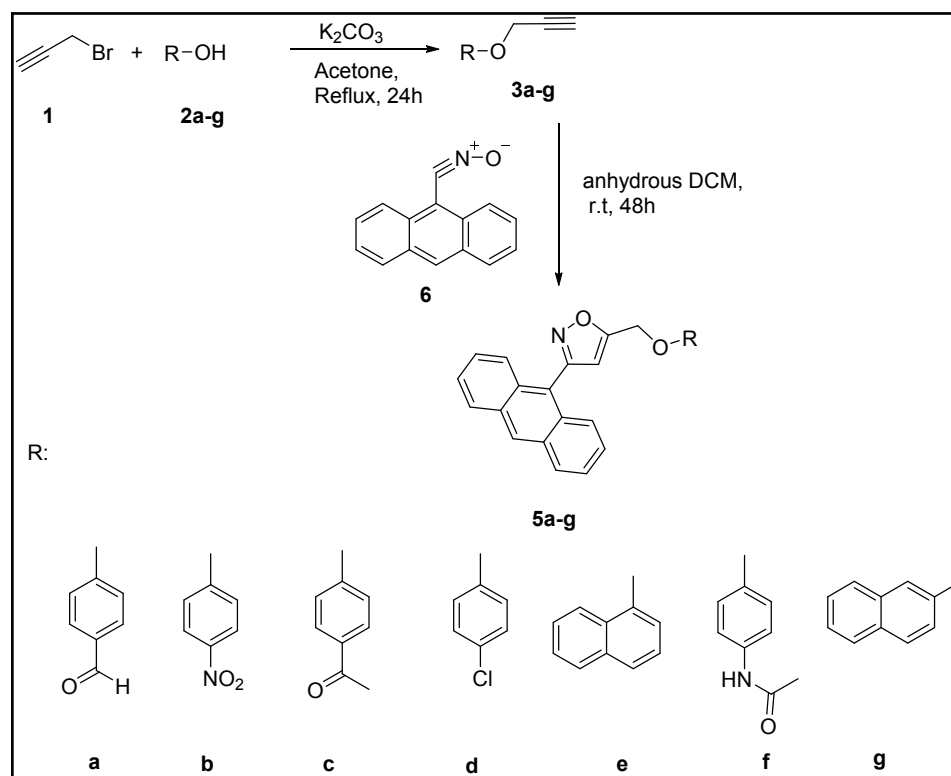
The synthesis and characterization of compounds 5a-g have been done by reacting of substituted ether via Nitrile Oxide. The chemical structures of the products 5a-g were established based on the IR, ^1H -NMR and ^{13}C -NMR spectral data (Table 1).

The results of the spectral analysis were in

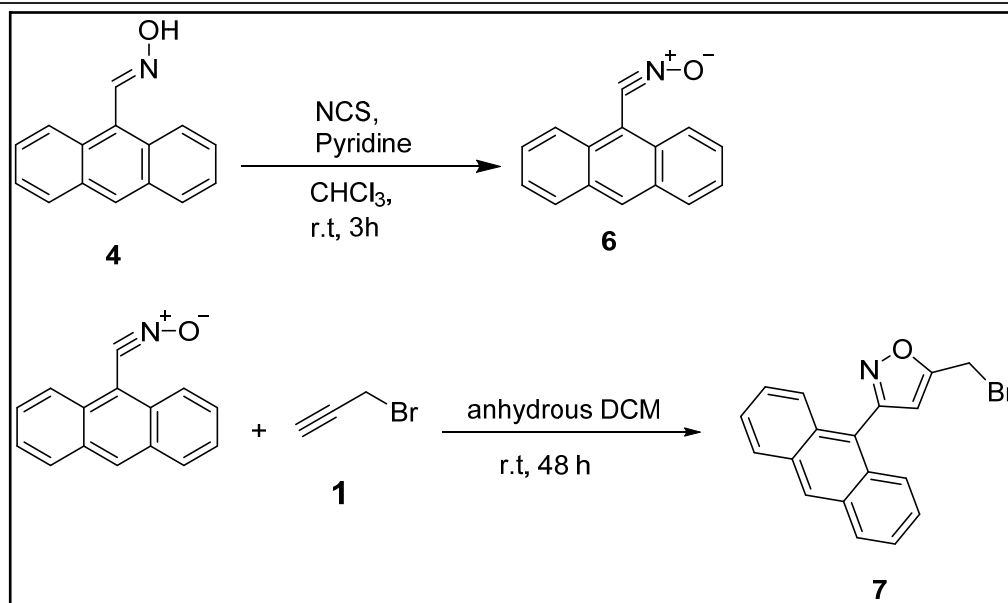
accordance with the proposed structures. The IR spectra of compounds 3a-g show that the absorption bands of the C-H stretching ranged at $3050\text{--}3158\text{ cm}^{-1}$ and C-O appeared between 1218 and 1265 cm^{-1} , with various yields of 57-94%. 9-anthracenenitrile oxide 6 has been used to react with compounds 3a-g to synthesise serious compounds of isoxazole derivatives 5a-g (Scheme 2).

Table 1 IR Spectral, physical and analytical data of compounds 5a-g

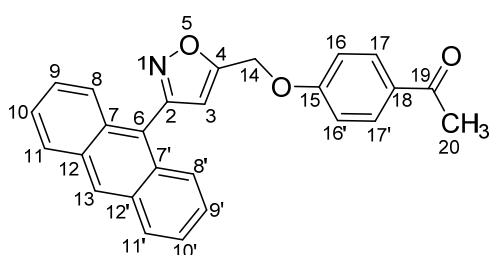
Comps	Chemical formula	(C-H)	(C-O)	(C=O)	Yield %	M.P °C	Colour
5a	$\text{C}_{25}\text{H}_{17}\text{NO}_3$	3124	1238	1689	92	109-111	Yellow
5b	$\text{C}_{24}\text{H}_{16}\text{N}_2\text{O}_4$	3158	1249	-----	94	101-103	Yellow
5c	$\text{C}_{26}\text{H}_{19}\text{NO}_3$	3120	1245	1666	82	121-123	Dark yellow
5d	$\text{C}_{24}\text{H}_{16}\text{ClNO}_2$	3135	1230	-----	89	107-109	Pale yellow
5e	$\text{C}_{28}\text{H}_{19}\text{NO}_2$	3050	1257	-----	57	110-112	Orange
5f	$\text{C}_{28}\text{H}_{20}\text{N}_2\text{O}_3$	3131	1218	1658	72	138-140	Gray
5g	$\text{C}_{28}\text{H}_{19}\text{NO}_2$	3050	1265	-----	65	143-145	Pale yellow



Scheme 2 Synthesis of oxyprop-1-yne 3a-g and (3-(anthracen-9-yl) isoxazol-5-yl) derivatives 5a-g

**Scheme 3** Synthesis of 3-(anthracen-9-yl)-5-(bromomethyl) isoxazole 7**Table 2** ^1H -NMR and APT ^{13}C -NMR chemical shift assignments in ppm for synthesized compounds 5a-f

Compds	^1H -NMR and APT ^{13}C -NMR chemical shifts in ppm
<p>5a</p>	<p>^1H-NMR (600 MHz, $\text{DMSO}-d_6$, 25°C): d = 5.64 (s, 2H, $\text{C}_{14}\text{-H}_2$), 7.08 (s, 1H, $\text{C}_3\text{-H}$), 7.36 (d, 2H, $J = 8.5$ Hz, $\text{C}_{16,16'}\text{-H}$), 7.56-7.58 (m, 4H, $\text{C}_{9,9'},_{10,10'}\text{-H}$), 7.70 (d, 2H, $J = 8.5$ Hz, $\text{C}_{17,17'}\text{-H}$), 7.95 (d, 2H, $J = 8.5$ Hz, $\text{C}_{11,11'}\text{-H}$), 8.19 (d, 2H, $J = 8.3$ Hz, $\text{C}_{8,8'}\text{-H}$), 8.82 (s, 1H, $\text{C}_{13}\text{-H}$), 9.92 (s, 1H, $\text{C}_{19}\text{-H}$).</p> <p>APT^{13}C-NMR (150 MHz, $\text{DMSO}-d_6$, 25°C): δ C: Upside (108.38: C_3, 115.87: $\text{C}_{16,16'}$, 125.37: $\text{C}_{9,9'}$, 126.12: $\text{C}_{10,10'}$, 127.46: $\text{C}_{11,11'}$, 129.14: $\text{C}_{8,8'}$, 131.10: C_{13}, 132.32: $\text{C}_{17,17'}$) Downside: (61.33: C_{14}, 126.15: $\text{C}_{7,7'}$, 127.50: $\text{C}_{12,12'}$, 131.14: C_{18}, 132.28: C_6, 160.83: C_2, 162.87: C_{15}, 168.37: C_4, 191.90: C_{19})</p>
<p>5b</p>	<p>^1H-NMR (600 MHz, $\text{DMSO}-d_6$, 25°C): d = 5.67 (s, 2H, $\text{C}_{14}\text{-H}_2$), 7.36 (s, 1H, $\text{C}_3\text{-H}$), 7.37-7.39 (d, 2H, $\text{C}_{16,16'}\text{-H}$), 7.54-7.58 (m, 4H, $\text{C}_{9,9'},_{10,10'}\text{-H}$), 7.69-7.71 (d, 2H, $\text{C}_{8,8'}\text{-H}$), 8.17-8.2 (d, 2H, $\text{C}_{11,11'}\text{-H}$), 8.26 - 8.29 (d, 2H, $\text{C}_{17,17'}\text{-H}$), 8.81 (s, 1H, $\text{C}_{13}\text{-H}$).</p> <p>APT ^{13}C-NMR (150 MHz, $\text{DMSO}-d_6$, 25°C): δ C: Upside: (108.48: C_3, 115.99: $\text{C}_{16,16'}$, 125.38: $\text{C}_{9,9'}$, 126.36: $\text{C}_{17,17'}$, 127.49: $\text{C}_{10,10'}$, 129.13: $\text{C}_{11,11'}$, 130.34: $\text{C}_{8,8'}$, 131.13: C_{13}) Downside: 61.74: C_{14}, 126.39: $\text{C}_{7,7'}$, 127.4: $\text{C}_{12,12'}$, 129.0: C_{15}, 142.01: C_6, 160.86: C_2, 163.18: C_{18}, 168.05: C_4</p>

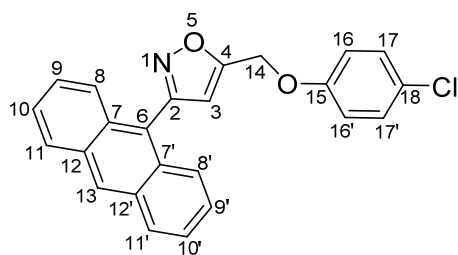
**5c**

¹H-NMR (600 MHz, DMSO-*d*₆, 25°C): δ = 2.53 (s, 3H, C₂₀-H₃), 5.61 (s, 2H, C₁₄-H₂), 7.06 (s, 1H, C₃-H), 7.25 (d, 2H, *J* = 7.6 Hz, C_{16,16'}-H), 7.52-7.54 (m, 4H, C_{9,9'}, C_{10,10'}-H), 7.73 (d, 2H, *J* = 7.4 Hz, C_{17,17'}-H), 7.99 (d, 2H, *J* = 7.6 Hz, C_{11,11'}-H), 8.16 (d, 2H, *J* = 7.2 Hz, C_{8,8'}-H), 8.77 (s, 1H, C₁₃-H).

APT ¹³C-NMR (150 MHz, DMSO-*d*₆, 25°C): δ C:

Upside: (25.88: C₂₀, 108.28: C₃, 115.17: C_{16,16'}, 125.40: C_{9,9'}, 126.10: C_{10,10'}, 127.45: C_{11,11'}, 129.11: C_{8,8'}, 130.35: C₁₃, 130.95: C_{17,17'})

Downside: 61.24: C₁₄, 125.37: C_{7,7'}, 126.07: C_{12,12'}, 129.07: C₁₈, 130.98: C₆, 160.85: C₂, 161.78: C₁₅, 168.52: C₄, 196.79: C₁₉

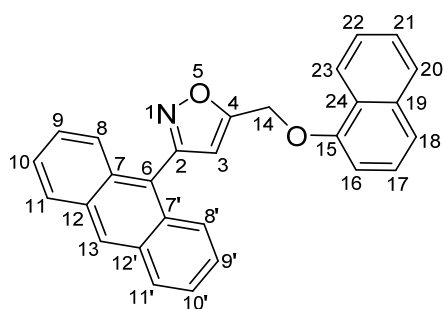
**5d**

¹H-NMR (600 MHz, DMSO-*d*₆, 25°C): δ = 5.5 (s, 2H, C₁₄-H₂), 7.01 (s, 1H, C₃-H), 7.18 (d, 2H, *J* = 8.8 Hz, C_{16,16'}-H), 7.40 (d, 2H, *J* = 8.8 Hz, C_{17,17'}-H), 7.52-7.58 (m, 4H, C_{9,9'}, C_{10,10'}-H), 7.70 (d, 2H, *J* = 8.3 Hz, C_{11,11'}-H), 8.17 (d, 2H, *J* = 8.3 Hz, C_{8,8'}-H), 8.79 (s, 1H, C₁₃-H).

APT ¹³C-NMR (150 MHz, DMSO-*d*₆, 25°C): δ C:

Upside: (108.20: C₃, 117.32: C_{16,16'}, 125.40: C_{9,9'}, 126.11: C_{10,10'}, 127.41: C_{17,17'}, 129.84: C_{11,11'}, 130.34: C_{8,8'}, 131.12: C₁₃)

Downside: 61.4: C₁₄, 125.36: C_{7,7'}, 127.44: C_{12,12'}, 129.86: C₁₅, 131.0: C₆, 156.90: C₂, 160.78: C₁₈, 168.72: C₄

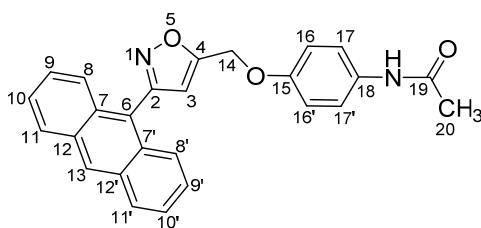
**5e**

¹H-NMR (600 MHz, DMSO-*d*₆, 25°C): δ = 5.63 (s, 2H, C₁₄-H₂), 7.1 (s, 1H, C₃-H), 7.34 (d, 2H, *J* = 8.8 Hz, C₁₆-H), 7.40 (t, 1H, *J* = 7.3 Hz, C₁₇-H), 7.51 (t, 2H, *J* = 7.3 Hz, C_{21,22}-H), 7.56-7.61 (m, 4H, C_{9,9'}, C_{10,10'}-H), 7.70 (d, 2H, *J* = 8.6 Hz, C_{11,11'}-H), 7.86-7.92 (m, 3H, C_{18,20,23}-H), 8.19 (d, 2H, *J* = 8.3 Hz, C_{8,8'}-H), 8.82 (s, 1H, C₁₃-H).

APT ¹³C-NMR (150 MHz, DMSO-*d*₆, 25°C): δ C:

Upside: (108.29: C₃, 119.06: C₁₆, 124.53: C₁₈, 125.40: C₂₃, 126.14: C_{9,9'}, 127.07: C₁₇, 127.29: C_{21,22}, 127.42: C_{10,10'}, 128.07: C_{11,11'}, 129.12: C₂₀, 130.07: C_{8,8'}, 131.12: C₁₃)

Downside: 61.21: C₁₄, 125.4: C₂₄, 126.1: C_{7,7'}, 127.45: C_{12,12'}, 129.47: C₆, 130.32: C₁₉, 155.90: C₂, 160.77: C₁₅, 168.95: C₄

**5f**

¹H-NMR (600 MHz, DMSO-*d*₆, 25°C): δ = 2.53 (s, 3H, C₂₀-H₃), 4.89 (s, 1H, NH), 5.61 (s, 2H, C₁₄-H₂), 7.06 (s, 1H, C₃-H), 7.25 (d, 2H, *J* = 7.3 Hz, C_{16,16'}-H), 7.52-7.54 (m, 4H, C_{9,9'}, C_{10,10'}-H), 7.73 (d, 2H, *J* = 7.3 Hz, C_{17,17'}-H), 7.99 (d, 2H, *J* = 7.7 Hz, C_{11,11'}-H), 8.15 (d, 2H, *J* = 7.2 Hz, C_{8,8'}-H), 8.77 (s, 1H, C₁₃-H).

APT ¹³C-NMR (150 MHz, DMSO-*d*₆, 25°C): δ C:

Upside: (30.98: C₂₀, 108.28: C₃, 115.17: C_{16,16'}, 125.40: C_{9,9'}, 126.10: C_{10,10'}, 127.45: C_{11,11'}, 129.11: C_{8,8'}, 130.35: C₁₃, 130.95: C_{17,17'})

Downside: 61.24: C₁₄, 125.37: C_{7,7'}, 126.07: C_{12,12'}, 129.07: C₁₈, 130.98: C₆, 160.85: C₂, 161.78: C₁₅, 168.52: C₄, 196.79: C₁₉

Synthesis of amine functionalized isoxazoles

3-(anthracen-9-yl)-5-(bromomethyl) isoxazole 7 was used to react with different

amine derivatives to prepare isoxazole nitrogen based 9a-c in one simple step by using dimethyl sulfoxide and sodium bicarbonate (Scheme 4, Table 3).

Table 3 IR Spectral, physical and analytical data of compounds 9a-c

Comps	Chemical formula	(N-H)	(C-H)	Yield %	M.P °C	Colour
9a	C ₂₄ H ₁₇ N ₃ O ₃	3378	3120	65	181-183	Yellow
9b	C ₂₄ H ₁₇ BrN ₂ O	3309	3131	73	137-139	White
9c	C ₂₄ H ₁₇ ClN ₂ O	3340	3139	68	241-243	White

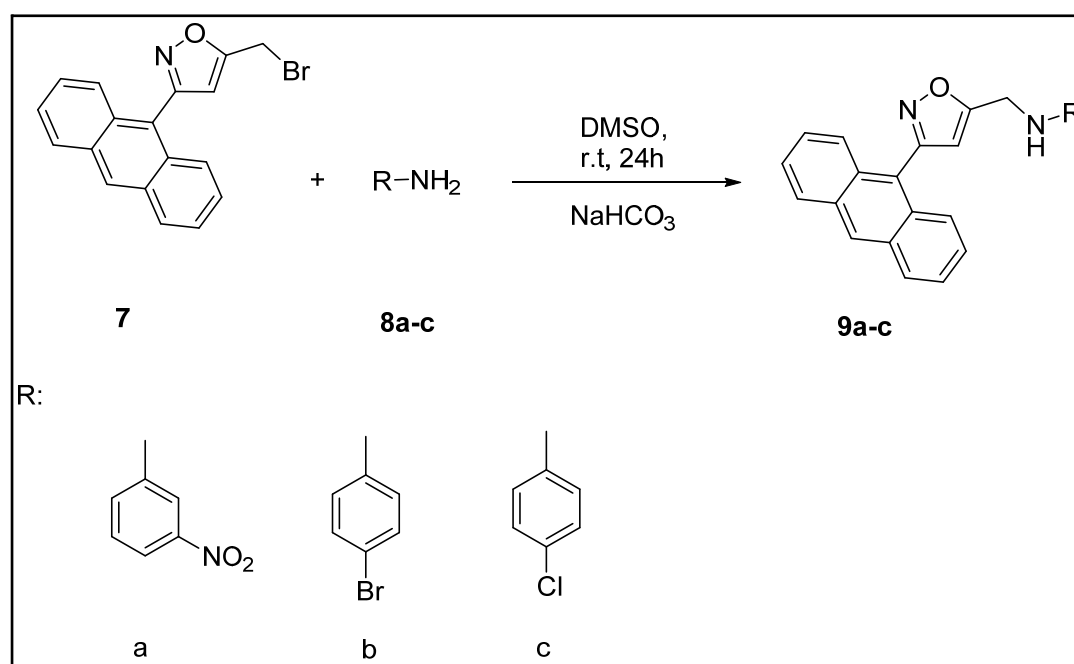
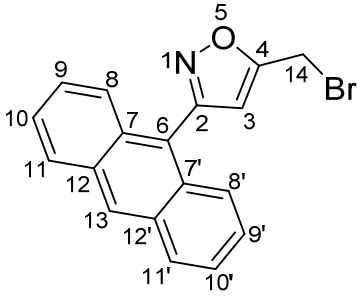
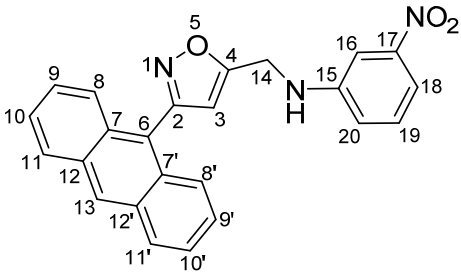
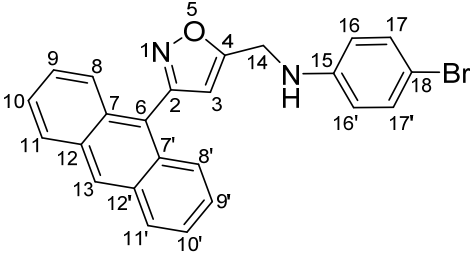
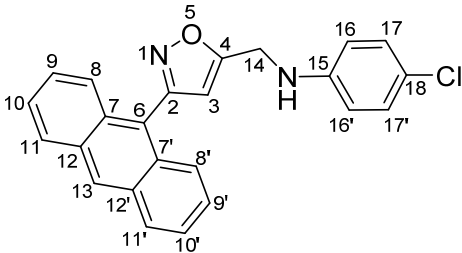
**Scheme 4** Synthesis of 1-(3-(anthracen-9-yl) isoxazol-5-yl)-N- analogue 9a-c

Table 4 ^1H -NMR and APT ^{13}C -NMR chemical shift assignments in ppm for synthesized compounds 9a-c

Comps	^1H -NMR and APT ^{13}C -NMR chemical shifts in ppm
 <p style="text-align: center;">7</p>	<p>^1H-NMR (600 MHz, $\text{DMSO}-d_6$, 25°C): d = 4.68 (s, 2H, $\text{C}_{14}\text{-H}_2$), 5.59 (s, 1H, $\text{C}_3\text{-H}$), 7.47-7.54 (m, 4H, $\text{C}_{9,9'},_{10,10'}\text{-H}$), 7.85-7.78 (m, 4H, $\text{C}_{11,11'}\text{-H}$), 8.05-8.08 (m, 2H, $\text{C}_{8,8'}\text{-H}$), 8.59 (s, 1H, $\text{C}_{13}\text{-H}$)</p> <p>^{13}C-NMR (150 MHz, $\text{DMSO}-d_6$, 25°C): δ C: (18.6: C_{14}, 107.2: C_3, 122.4: $\text{C}_{9,9'}$, 125.0: $\text{C}_{10,10'}$, 125.3: $\text{C}_{7,7'}$, 125.4: $\text{C}_{11,11'}$, 126.6: $\text{C}_{8,8'}$, 128.5: C_{13}, 129.1: $\text{C}_{12,12'}$, 131.0: C_6, 161.2: C_2, 167.8: C_4)</p>
 <p style="text-align: center;">9a</p>	<p>^1H-NMR (600 MHz, $\text{DMSO}-d_6$, 25°C): d = 4.80 (s, 2H, $\text{C}_{14}\text{-H}_2$), 6.78 (s, 1H, $\text{C}_3\text{-H}$), 7.21 (bs, 2H, $\text{C}_{16}\text{-H}$, NH), 7.41 (t, 1H, $J = 8$ Hz, $\text{C}_{19}\text{-H}$), 7.45-7.51 (m, 2H, $\text{C}_{20,18'}\text{-H}$), 7.54-7.61 (m, 4H, $\text{C}_{9,9'},_{10,10'}\text{-H}$), 7.69 (d, 2H, $J = 8.6$ Hz, $\text{C}_{11,11'}\text{-H}$), 8.156 (d, 2H, $J = 8.4$ Hz, $\text{C}_{8,8'}\text{-H}$), 8.78 (s, 1H, $\text{C}_{13}\text{-H}$)</p> <p>APT ^{13}C-NMR (150 MHz, $\text{DMSO}-d_6$, 25°C): δ C:</p> <p>Upside: (106.48: C_3, 111.42: C_{20}, 119.46: C_{16}, 125.43: C_{18}, 126.09: $\text{C}_{9,9'}$, 127.25: $\text{C}_{10,10'}$, 129.06: $\text{C}_{11,11'}$, 130.2: $\text{C}_{8,8'}$, 130.56: C_{13}, 131.1: C_{19})</p> <p>Downside: 39.30: C_{14}, 126.0: C_{17}, 127.29: $\text{C}_{7,7'}$, 131.11: $\text{C}_{12,12'}$, 149.29: C_6, 149.51: C_2, 164.6: C_{15}, 171.61: C_4)</p>
 <p style="text-align: center;">9b</p>	<p>^1H-NMR (600 MHz, $\text{DMSO}-d_6$, 25°C): d = 4.66 (s, 2H, $\text{C}_{14}\text{-H}_2$), 6.64-6.75 (m, 4H, $\text{C}_{16,16'},_{17,17'}\text{-H}$), 7.28 (d, 2H, $J = 8.5$ Hz, $\text{C}_3\text{-H}$, NH), 7.50-7.57 (m, 4H, $\text{C}_{9,9'},_{10,10'}\text{-H}$), 7.69 (d, 2H, $J = 8.2$ Hz, $\text{C}_{11,11'}\text{-H}$), 8.16 (d, 2H, $J = 8.1$ Hz, $\text{C}_{8,8'}\text{-H}$), 8.77 (s, 1H, $\text{C}_{13}\text{-H}$)</p> <p>APT ^{13}C-NMR (150 MHz, $\text{DMSO}-d_6$, 25°C): δ C:</p> <p>Upside: (106.26: C_3, 115.10: $\text{C}_{16,16'}$, 125.45: $\text{C}_{9,9'}$, 126.09: $\text{C}_{10,10'}$, 127.29: $\text{C}_{11,11'}$, 129.08: $\text{C}_{8,8'}$, 130.28: C_{13}, 131.92: $\text{C}_{17,17'}$)</p> <p>Downside: 39.47: C_{14}, 125.49: C_{18}, 126.0: $\text{C}_{7,7'}$, 129.0: $\text{C}_{12,12'}$, 131.95: C_6, 147.70: C_{15}, 160.55: C_2, 172.18: C_4)</p>
 <p style="text-align: center;">9c</p>	<p>^1H-NMR (600 MHz, $\text{DMSO}-d_6$, 25°C): d = 4.67 (s, 2H, $\text{C}_{14}\text{-H}_2$), 6.67-6.75 (m, 4H, $\text{C}_{16,16'},_{17,17'}\text{-H}$), 7.28 (d, 2H, $J = 8.4$ Hz, $\text{C}_3\text{-H}$, NH), 7.49-7.56 (m, 4H, $\text{C}_{9,9'},_{10,10'}\text{-H}$), 7.70 (d, 2H, $J = 8.3$ Hz, $\text{C}_{11,11'}\text{-H}$), 8.15 (d, 2H, $J = 8.1$ Hz, $\text{C}_{8,8'}\text{-H}$), 8.75 (s, 1H, $\text{C}_{13}\text{-H}$)</p> <p>APT ^{13}C-NMR (150 MHz, $\text{DMSO}-d_6$, 25°C): δ C:</p> <p>Upside: (106.26: C_3, 115.10: $\text{C}_{16,16'}$, 125.50: $\text{C}_{9,9'}$, 126.07: $\text{C}_{10,10'}$, 127.28: $\text{C}_{11,11'}$, 129.07: $\text{C}_{8,8'}$, 130.1: C_{13}, 131.92: $\text{C}_{17,17'}$)</p> <p>Downside: 39.48: C_{14}, 125.3: C_{18}, 126.0: $\text{C}_{7,7'}$, 128.9: $\text{C}_{12,12'}$, 131.96: C_6, 147.70: C_{15}, 160.56: C_2, 172.18: C_4)</p>

Biological Activity

The antibacterial and antifungal activities of the synthesised compounds were examined in vitro. Gram-positive bacteria (*Staphylococcus aureus*) and Gram-negative bacteria (*Escherichia coli*) were used for this screening. The antifungal activity of each synthesised isoxazole derivative was examined in vitro against *Candida albicans*. The zone of inhibition produced by each compound was measured in mm in an incubator for 24 hrs. at 37°C (Table 5).

Compounds 5a-e exhibited various antibacterial activity against *Escherichia coli* as gram-negative bacteria ranging from 21 to 40 mm of the inhibitory zone (30 µg), indicating a positive antibacterial influence on all synthesised compounds. However, compounds 5a and 5f show maximum inhibition zone at 13 and 14 ppm, respectively.

Antioxidant activity

This section aimed to evaluate the antioxidant activity of the prepared new compounds 5a-f in this study. There is a growing importance of antioxidants especially substituted phenols to prevent cell damage and treatment of skin diseases.⁽²⁷⁾

It is essential to choose and use a quick and stable method to evaluate antioxidant activity for avoiding the time-consuming task of evaluating hundreds of compounds.⁽²⁸⁾ There are many methods to measure the antioxidant activity of molecules. The most general and dependable method includes the evaluation of the antioxidant activity using a spectrophotometer, such as 1,1-diphenyl-2-picrylhydrazyl radical (DPPH), which was reported by Brand-Williams *et al.*⁽²⁹⁾

Reduction of (DPPH) by a radical species (R),
 $\text{DPPH}^\cdot + \text{R}^\cdot \rightarrow \text{DPPH-R}$ or using an antioxidant (AH), $\text{DPPH}^\cdot + \text{AH} \rightarrow \text{DPPH-H} + \text{A}^\cdot$, this led to the loss of absorbance at around 515 nm.⁽³⁰⁾

When the prepared compounds with the DPPH solution were left for a period of time, a colour change was observed only in 5e among these compounds, and the rest of the compounds kept their violet colour. This indicates the structure of the compound 5e plays an important role in terms of antioxidant activity because merely is not able to donate a proton. Therefore, this activity was measured in triplicate only for 5e by using the 1,1-diphenyl-2-picrylhydrazyl radical (DPPH),

Table 5 Antibacterial and antifungal activities of synthesized compounds 5a-e and 9a-c

Compds	<i>Escherichia coli</i>			<i>Staphylococcus aureus</i>			<i>Candida albicans</i>
	5 µg	15 µg	30 µg	5 µg	15 µg	30 µg	400 ppm
5a	14	21	30	----	----	----	12
5b	20	25	38	----	----	----	7
5c	16	25	32	----	----	----	----
5d	17	22	28	11	15	18	6
5e	11	15	21	----	----	10	13
5f	----	----	----	----	----	----	14
9a	31	35	40	----	----	----	8
9b	14	16	27			30	9
9c	5	9	17			18	----

which exhibited an excellent antioxidant activity (97.8 %) as shown in (Figure 1).

Molecular Docking study

The correct absorption and binding between the drug and the receptor are referred to as molecular docking. The most significant interaction between a ligand and receptor is the lowest docking energy. AutoDock vina was used for the evaluation

of the affinity between the synthesised compounds and selected receptors. Among multiple docking poses, just the highest docking scores were included in the study. All the data regarding the binding force, the number of hydrogen bonds interaction and amino acids' participation in the interactions are listed in (Table 6).

Table 6 In silico molecular docking results of 5a-f and 9a-c interaction with antidiabetic receptors

comps	(PDB ID: 1ai9)	pKi (μM)	(PDB ID: 1bag)	pKi (μM)	(PDB ID: 1hnj)	pKi (μM)	(PDB ID: 1ea1)	pKi (μM)	(PDB ID: 2x08)	pKi (μM)
	Binding Energy (ΔG) (kcal/mol)		Binding Energy (ΔG) (kcal/mol)		Binding Energy (ΔG) (kcal/mol)		Binding Energy (ΔG) (kcal/mol)		Binding Energy (ΔG) (kcal/mol)	
5a	-9.6	6.94	-10.5	7.3	-9.2	6.8	-11.7	7.9	-11.2	7.64
5b	-9.4	6.9	-10.2	7.2	-8.3	6.4	-10.9	7.5	-10.9	7.5
5c	-9.5	6.9	-10.1	7.15	-9.2	6.8	-10.7	7.4	-11.2	7.6
5d	-9.6	6.94	-9.9	7.1	-9.3	6.8	-10.6	7.4	-11.6	7.8
5e	-10.2	7.2	-10.9	7.5	-10.4	7.3	-12.8	8.3	-13.7	8.7
5f	-10.2	7.2	-10.5	7.3	-9.2	6.8	-11.9	7.94	-11.6	7.8
9a	-10.3	7.24	-10	7.11	-9.7	7	-10.7	7.4	-11.6	7.8
9b	-9.6	6.94	-10.2	7.2	-9.3	6.8	-11.3	7.7	-10.9	7.5
9c	-9.5	6.9	-10.1	7.15	-9.4	6.9	-11.7	7.9	-11.6	7.8



Figure 1 Antioxidant activity of compound 5e detected by change of color

In order to understand the mode of binding, molecular modelling and docking studies of the most potent inhibitors from each category, all synthesized compounds, were carried out within the active site of *Candida albicans* dihydrofolate reductase (PDB ID:1AI9) for antifungal, Alpha-amylase from *Bacillus subtilis* (PDB ID: 1BAG), and beta-ketoacyl-ACP synthase-III (PDB ID:1HNJ) for antibacterial, alpha-sterol demethylase (CYP51) from *M. Tuberculosis* (PDB ID: 1EA1) for antitubercular activities, and cytochrome c peroxidase (PDB ID: 2X08) for anti-oxidant activity.

The highest affinity value was -10.2

kcal/mol for 5a docking with *Candida albicans* dihydrofolate reductase (PDB ID: 1ai9). A hydrogen bond was conserved for the interaction of 5e with THR A:58. Further hydrophobic interactions were indicated with ILE A:19, MET A:25, ILE A: 33, and PHE A: 36, confirming the antifungal activity.

Compound 5e displayed the lowest energy of -10.9 kcal/mol with Alpha-amylase from *Bacillus subtilis* (PDB ID: 1bag) via interaction with hydrophobic bonds with LEU A 210, HIS A: 180, ALA A: 170, LEU A: 141, LEU A: 142, LEU A: 144, and TYR A: 59 (Figure 2).

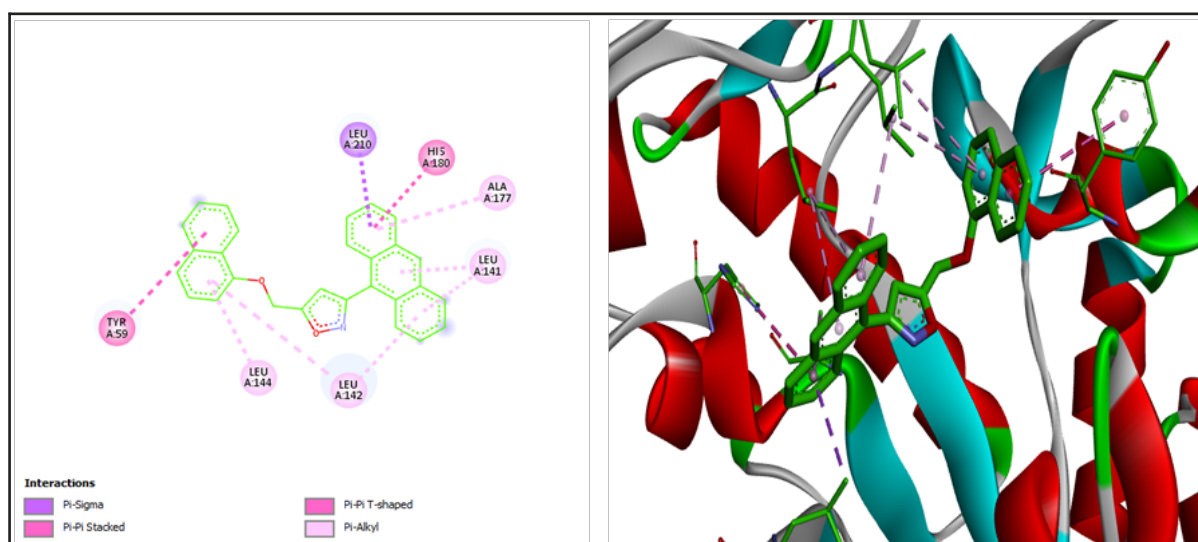


Figure 2 2D and 3D representation of the interaction of 5e with Alpha-amylase from *Bacillus subtilis* (PDB ID: 1bag)

Similarly, compound 5e showed a high binding site of -10.4 kcal/mol with beta-ketoacyl-ACP synthase-III (PDB ID:1HNJ). Amino acids that contributed to the bonding are: ASN A: 247, ASN A: 274, and ALA A: 246 which formed hydrogen bonds. Hydrophobic bonds were observed with VAL A: 212, LEU A: 189, GLY A: 209, MET A: 207, ILE A 156, ALA A 216, CYS A: 112, and ASN A: 210.

The lowest free energy of -12.8 kcal/mol was observed for the interaction of compounds 5e with alpha-sterol demethylase (CYP51) from *M. Tuberculosis* (PDB ID: 1EA1) for antitubercular activities via THR A:260, CYS A: 394, and GLY A: 398 as hydrogen bonds. Hydrophobic bonds have also been observed during interaction of 5e with alpha-sterol demethylase (CYP51) via amino acids of LEU A: 321, LEU A: 315, LEU A: 100, LEU A: 152, LEU A 105, PRO

A: 320, ALA A: 400, ALA A: 256, and ALA A: 104, respectively confirmed the highest antioxidant activity.

Compound 5e has also shown the highest affinity interaction score of -13.7 kcal/mol, with cytochrome c peroxidase (PDB ID: 2X08) and formed a Hydrophobic bond with VAL A: 45, ARG A: 48, HIS A: 175, ALA A: 174, MET A: 172, TRP A: 51, and LEU A: 171 (Figure 3).

To validate the current docking investigation at the active site, the co-crystallized ligand ascorbic acid was re-docked into the active site using the same set of parameters. The energy score was -5.9 Kcal/mol, indicating that the binding was valid. Ascorbic acid established four hydrogen bonds with the amino acids LYS A: 179, PRO A: 44, ARG A 184, and ARG A: 48.

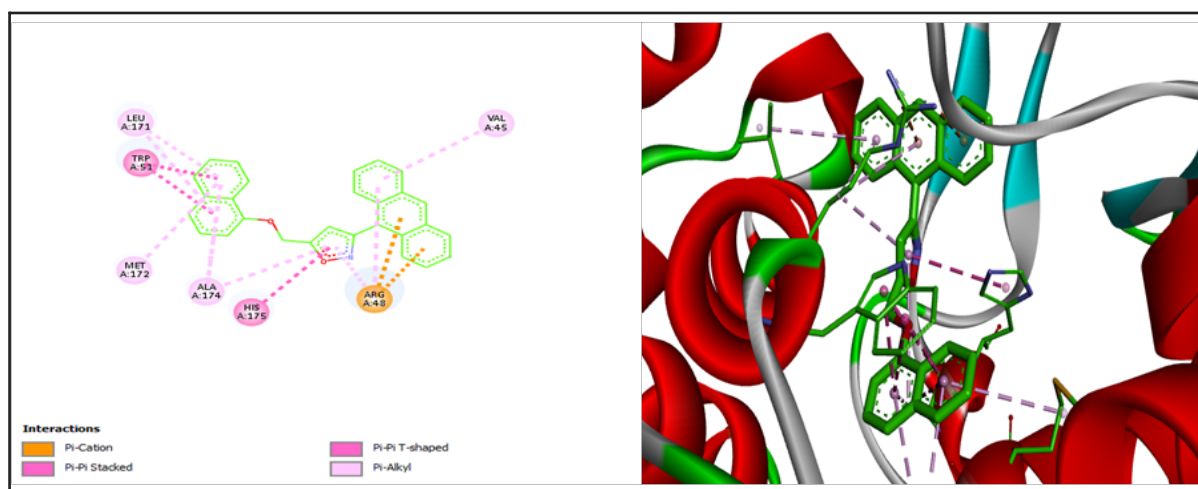
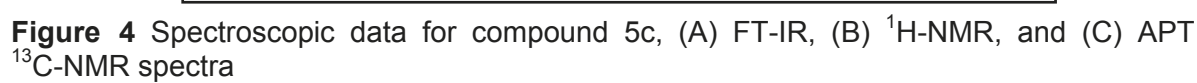


Figure 3 2D and 3D representation of the interaction of 5e with cytochrome c peroxidase (PDB ID: 2X08)



Discussion

In the present study, our team designed and synthesised a series of compounds 5a-g and 9a-c. Compounds 2a-g have been utilised as main intermediates to successfully achieve the substitution at the hydroxyl group to prepare ether with different substituents to the prop-2-yn-1-yloxy analogues. The absorption band of C-H stretching of propargyl ether at 3201-3281 cm^{-1} was observed by confirming new compounds 3a-g. The examination of the TLC of the reaction mixtures indicated the presence of only one product.

Compounds 3a-g were subjected to react with Nitrile Oxide via 1,3- dipolar cycloaddition reaction to prepare compounds 5a-g. The IR spectra of C-H stretching of propargyl ether for compounds 5a-g disappeared. The C-H stretching of isoxazole appeared at 3050-3158 cm^{-1} , showing the preparation of new compounds of 5a-g. In addition, distinct ν (C-O) bands were found in the range of 1218-1265 cm^{-1} . Absorption bands for C=O were revealed at 1689, 1666 and 1658 cm^{-1} for compounds 5a, 5c and 5f, respectively. All synthesised compounds 5a-g were confirmed by the new singlet peaks presence in ^1H - NMR centring around δ 7.01-7.36 ppm for hydrogen of (C-H) at carbon 3. This value of the chemical shift clearly confirms the regioselectivity of the cycloaddition reaction. Based on the integration values, the numbers of protons are in agreement with the proposed values. The ^{13}C NMR spectra of 5a-g showed two distinct sets of aromatic carbon and saturated carbon signals. The aromatic carbon signals of the anthracene group were found in the range of δ 125.3 to 131.1 ppm. The three carbons numbered 3, 2 and 4 signals for the isoxazole ring of compounds 5a-g were located in a region centering around δ 108, 60 and 168 ppm, respectively.

In addition, the NH stretching absorption bands for compounds 9a-c were revealed in the range of 3309-3378 cm^{-1} and the C-H stretching of the isoxazole ring was

observed at 3120, 3131 and 3139 cm^{-1} for compounds 9a-c. The N-H Stretching band of the 9a-c proton appeared as a broad singlet centring on δ = 7.21-7.29 ppm.

The nature and position of the substituents on the phenyl ring- O- and N-substituted for compounds 5a-f and 9a-c played a crucial role in the antifungal, antibacterial, anti-tuberculosis and antioxidant activities. The lowest binding energy scores and high affinity of -10.2, -10.2 and -10.3 Kcal/mol, bound to the active site of *Candida albicans* dihydrofolate reductase (PDB ID:1AI9) for antifungal, were observed for compounds 5e, 5f and 9a, respectively. Carbonaromatic ring might influence on the binding affinity of synthesized compounds 5e, 5f and 9a with *Candida albicans* dihydrofolate reductase (PDB ID:1AI9).

There is a compatibility between practical values and free energy values in the docking studies for antibacterial activity and antioxidant activity. Compounds 5b and 5d had electron-withdrawing groups (NO_2 and Cl) substituted at position 3 on the aromatic ring. The Nitro substituted at meta position was found to have better antibacterial activity compared with the Bromo group substituted at the para position. The chlorine substituted on the Phenyl ring - O-substituted for compound 9c was shown to have the inhibition zone of 17 mm compared to the bromine substituent of 27 mm substituted at the same position 3, and the Nitro group at position 2 on phenyl-o-substituted with the inhibition of 40 mm. Naphthalene substituent on the O-phenyl substituted by 5e exhibited the affinity in silico with Alpha-amylase from *Bacillus subtilis* (PDB ID: 1BAG), and beta-ketoacyl-ACP synthase-III (PDB ID:1HNJ) for antibacterial through hydrophobic bonds, hydrogen and hydrophobic bonds, respectively.

Compound 5e displayed the most effective anti-tuberculosis in silico to predict the highest binding site energy with alpha-sterol demethylase (CYP51) from *M. Tuberculosis* (PDB ID: 1EA1) followed by

compound 5f. All the synthesized compounds showed good to moderate activities for antioxidants based on the docking binding site energy with cytochrome peroxidase (PDB ID: 2X08). However, only compound 5e demonstrated a colour change during the experimental antioxidant procedure. Naphthalene moiety has been found to improve the pharmacological activity and metabolic stability of the active molecule.

Conclusion

In this study, been synthesized based on oxygen and nitrogen substituted on Isoxazole derivatives via Nitrile Oxide, 1,3-dipolar cycloaddition reaction. It was found that most of the synthesised compounds are active against the tested cell lines. Nitro substituted on meta position 9a was found to have better antibacterial compared with the bromo and chloro-group substituted 9b and 9c at the para position, respectively. The compounds with naphthalene and chlorophenyl substituted have the highest antibacterial activity. Compound 5e substituted with Naphthalene moiety exhibited effective radical scavenging abilities based on docking binding site energy and antioxidant using a UV-visible spectrophotometer.

Competing interests

The authors declare that they have no competing interests.

References

1. Zhu J, Mo J, Lin HZ, Chen Y, Sun HP. The recent progress of isoxazole in medicinal chemistry. *Bioorg Med Chem*. 2018; 26(12):3065-75. DOI:10.1016/j.bmc.2018.05.013.
2. Ahmed SM, Hussain FHS, Quadrelli P. 9-Anthraldehyde oxime: a synthetic tool for variable applications. *Monatsh fur Chem*. 2020; 151:1643-58. DOI:10.1007/s00706-020-02695-2.
3. Rammah MM, Gati W, Mtiraoui H, Rammah MEB, Ciamala K, Knorr M, et al. Synthesis of Isoxazole and 1, 2, 3-Triazole Isoindole Derivatives via Silver-and Copper-Catalyzed 1, 3-Dipolar Cycloaddition Reactions. *Molecules*. 2016; 21(3):307. DOI:10.3390/molecules21030307.
4. Zhang H-K, Eaton JB, Fedolak A, Gunosewoyo H, Onajole OK, Brunner D, et al. Synthesis and biological evaluation of novel hybrids of highly potent and selective $\alpha 4 \beta 2$ -Nicotinic acetylcholine receptor (nAChR) partial agonists. *Eur J Med Chem*. 2016; 124:689-97. DOI:10.1016/j.ejmech.2016.09.016.
5. Sowmya D, Teja GL, Padmaja A, Prasad VK, Padmavathi V. Green approach for the synthesis of thiophenyl pyrazoles and isoxazoles by adopting 1, 3-dipolar cycloaddition methodology and their antimicrobial activity. *Eur J Med Chem*. 2018; 143:891-8. DOI: 10.1016/j.ejmech.2017.11.093.
6. Khodabandlou S, Saraei M. Synthesis of novel isoxazole derivatives bearing kojic acid moiety and evaluation of their antimicrobial activity. *Chem Heterocycl Compd*. 2021; 57:823-7. DOI:10.1007/s10593-021-02986-4.
7. Mączyński M, Borska S, Mieszala K, Kocięba M, Zaczynska E, Kochanowska I, et al. Synthesis, Immunosuppressive Properties, and Mechanism of Action of a New Isoxazole Derivative. *Molecules*. 2018; 23(7):1545. DOI:10.3390/molecules23071545.
8. Aksenov AV, Aksenov DA, Arutiunov NA, Aksenov NA, Aleksandrova EV, Zhao Z, et al. Synthesis of Spiro[indole-3,5'-isoxazoles] with Anticancer Activity via a Formal [4 + 1]-Spirocyclization of Nitroalkenes to Indoles. *J Org Chem*. 2019; 84(11):7123-37. DOI:10.1021/acs.joc.9b00808.
9. Bibi H, Nadeem H, Abbas M, Arif M. Synthesis and anti-nociceptive potential of isoxazole carboxamide derivatives. *BMC Chem*. 2019; 13(1):6. DOI:10.1186/s13065-019-0518-6.
10. Abdelall EKA. Synthesis and biological evaluations of novel isoxazoles and furoxan derivative as anti-inflammatory agents. *Bioorg Chem*. 2020; 94:103441. DOI:10.1016/j.bioorg.2019.103441.
11. Ahmed SM, Hussain FH, Leusciatti M, Mannucci B, Mella M, Quadrelli P. Phosphorylation of 10-bromoanthracen-9-yl-cyclopenta [d] isoxazol-6-ols: chemistry suitable for antivirals. *ARKIVOC*. 2022; 2022. DOI:10.24820/ark.55501.90.p011.784
12. Moiola M, Bova A, Crespi S, Memeo MG, Mella M, Overkleeft HS, et al. Fluorescent Probes from Aromatic Polycyclic Nitrile Oxides: Isoxazoles versus Dihydro-1 λ 3, 3, 2 λ 4-Oxazaborinines. *Chemistry Open*. 2019; 8(6):770-80. DOI:10.1002/open.201900137.
13. Begum S, Begum T, Rahman N, Khan RA. A review on antibiotic resistance and way of combating antimicrobial resistance. *GSC Biol Pharm Sci*. 2021; 14(2):087-97. DOI: 10.30574/gscbps.2021.14.2.0037.
14. Prakash B. Functional and preservative properties of phytochemicals: Academic Press; 2020.
15. Alós J-I. Resistencia bacteriana a los antibióticos: una crisis global. *Enferm Infecc Microbiol Clin*. 2015; 33(10):692-9. DOI: 10.1016/j.eimc.2014.10.004.

16. Raza A, Ngieng SC, Sime FB, Cabot PJ, Roberts JA, Popat A, et al. Oral meropenem for superbugs: challenges and opportunities. *Drug Discov Today*. 2021; 26(2):551-60. DOI: [10.1016/j.drudis.2020.11.004](https://doi.org/10.1016/j.drudis.2020.11.004).
17. Ahmed SM, Salih KM, Ahmad HO, Jawhar ZH, Hamad DH. Synthesis, spectroscopic characterization and antibacterial activity of new series of Schiff base derived from 4-aminoantipyrine and 2-amino benzimidazole. *Zanco J Med Sci*. 2019; 23(2):206-16. DOI: [10.15218/zjms.2019.026](https://doi.org/10.15218/zjms.2019.026)
18. Minuti LF, Memeo MG, Crespi S, Quadrelli P. Fluorescent Probes from Stable Aromatic Nitrile Oxides. *Eur J Org Chem*. 2016; 2016(4):821-9. DOI: [10.1002/ejoc.201501478](https://doi.org/10.1002/ejoc.201501478).
19. Memeo MG, Distanti F, Quadrelli P. (2S)-[3-(Anthracen-9-yl)-4, 5-dihydroisoxazol-5-yl] methyl 2-[(tert-butoxycarbonyl) amino] propanoate. *Molbank*. 2014; 2014(4):M837. DOI: [10.3390/M837](https://doi.org/10.3390/M837)
20. Castillo JC, Orrego-Hernández J, Portilla J. Cs₂CO₃-Promoted Direct N-Alkylation: Highly Chemoselective Synthesis of N-Alkylated Benzylamines and Anilines. *Eur J Org Chem*. 2016; 2016(22):3824-35. DOI: [10.1002/ejoc.201600549](https://doi.org/10.1002/ejoc.201600549)
21. Salih KM, Ameen D, Hamad AN, Ganjo AR, Muhammed S. Synthesis and pharmacological profile of some new 2-substituted-2, 3-dihydro-1H-perimidine. *Zanco J Med Sci*. 2020; 24(1):68-79. DOI: [10.15218/zjms.2020.010](https://doi.org/10.15218/zjms.2020.010)
22. GAUTAM KC, SINGH DP. Synthesis and antimicrobial activity of some isoxazole derivatives of thiophene. *Chem Sci Trans*. 2013; 2(3):992-6. DOI: [10.7598/cst2013.478](https://doi.org/10.7598/cst2013.478)
23. Garcia EJ, Oldoni TLC, Alencar SMd, Reis A, Loguercio AD, Grande RHM. Antioxidant activity by DPPH assay of potential solutions to be applied on bleached teeth. *Braz Dent J*. 2012; 23:22-7. DOI: [10.1590/S0103-64402012000100004](https://doi.org/10.1590/S0103-64402012000100004).
24. Pandey SK, Yadava U, Sharma M, Upadhyay A, Gupt MP, Dwivedi AR, et al. Synthesis, molecular structure investigation, biological evaluation and docking studies of novel spirothiazolidinones. *Results Chemistry*. 2023; 5:100726. DOI: [10.1016/j.rechem.2022.100726](https://doi.org/10.1016/j.rechem.2022.100726)
25. Obaid RJ. New benzimidazole derivatives: Design, synthesis, docking, and biological evaluation. *Arab J Chem*. 2023; 16(2):104505. DOI: [10.1016/j.arabjc.2022.104505](https://doi.org/10.1016/j.arabjc.2022.104505)
26. Ashraf SA, Elkhaila AEO, Mehmood K, Adnan M, Khan MA, Eltoum NE, et al. Multi-targeted molecular docking, pharmacokinetics, and drug-likeness evaluation of okra-derived ligand abscisic acid targeting signaling proteins involved in the development of diabetes. *Molecules*. 2021; 26(19):5957. DOI: [10.3390/molecules26195957](https://doi.org/10.3390/molecules26195957).
27. Abbott AP, Ahmed EI, Prasad K, Qader IB, Ryder KS. Liquid pharmaceuticals formulation by eutectic formation. *Fluid Ph Equilib*. 2017; 448:2-8. DOI: [10.1016/j.fluid.2017.05.009](https://doi.org/10.1016/j.fluid.2017.05.009).
28. Qader IB, Laguerre M, Lavaud A, Tenon M, Prasad K, Abbott AP. Selective Extraction of Antioxidants by Formation of a Deep Eutectic Mixture through Mechanical Mixing. *ACS Sustain Chem Eng*. 2023; 11(10):4168-76. DOI: [10.1021/acssuschemeng.2c06894](https://doi.org/10.1021/acssuschemeng.2c06894).
29. Santos AF, Argolo AC, Paiva PM, Coelho LC. Antioxidant activity of Moringa oleifera tissue extracts. *Phytother Res*. 2012; 26(9):1366-70. DOI: [10.1002/ptr.4591](https://doi.org/10.1002/ptr.4591)
30. Zheng L, Lin L, Su G, Zhao Q, Zhao M. Pitfalls of using 1, 1-diphenyl-2-picrylhydrazyl (DPPH) assay to assess the radical scavenging activity of peptides: Its susceptibility to interference and low reactivity towards peptides. *Food Res Int*. 2015; 76:359-65. DOI: [10.1016/j.foodres.2015.06.045](https://doi.org/10.1016/j.foodres.2015.06.045)